ARTICLE
Journal of Cellular Biochemistry 114:716–727 (2013)

Journal of Cellular Biochemistry

Autocrine Fibroblast Growth Factor 2-Mediated Interactions Between Human Mesenchymal Stem Cells and Extracellular Matrix Under Varying Oxygen Tension

Junho Kim and Teng Ma*

Department of Chemical and Biomedical Engineering, Florida State University, Tallahassee, Florida 32310

ABSTRACT

Human mesenchymal stromal or stem cells (hMSCs) are being investigated for cell therapy in a wide range of diseases. MSCs are a potent source of trophic factors and actively remodel their immediate microenvironment through the secretion of bioactive factors in response to external stimuli such as oxygen tension. In this study, we examined the hypothesis that hypoxia influences hMSC properties in part through the regulation of extracellular milieu characterized by the extracellular matrix (ECM) matrices and the associated fibroblast growth factor-2 (FGF-2). The decellularized ECM matrices derived from hMSC culture under both hypoxic (e.g., 2% O_2) and the standard culture (e.g., 20% O_2) conditions have different binding capacities to the cell-secreted and exogenenous FGF-2. The reduced hMSC proliferation in the presence of FGF-2 inhibitor and the differential capacity of the decellularized ECM matrices in regulating hMSC osteogeneic and adipogenic differentiation suggest an important role of the endogenous FGF-2 in sustaining hMSC proliferation and regulating hMSC fate. Additionally, the combination of the ECM adhesion and hypoxic culture preserved hMSC viability under serum withdrawal. Together, the results suggest the synergistic effect of hypoxia and the ECM matrices in sustaining hMSC ex vivo expansion and preserving their multi-potentiality and viability under nutrient depletion. The results have important implication in optimizing hMSC expansion and delivery strategies to obtain hMSCs in sufficient quantity with required potency and to enhance survival and function upon transplantation. J. Cell. Biochem. 114: 716–727, 2013.

KEY WORDS: MESENCHYMAL STEM CELLS; HYPOXIA; EXTRACELLULAR MATRIX; FIBROBLAST GROWTH FACTOR-2

Human mesenchymal stromal cells (hMSCs) have generated excitement in both scientific and clinical communities because of therapeutic prospects for many devastating diseases. These reparative adult stem cells can be readily isolated from a small tissue sample, expand in culture, and enhance tissue repair and regeneration through differentiation and/or paracrine actions [Pittenger et al., 1999]. MSCs are being tested in clinical trials ranging from bone and cartilage repair to ischemic heart and cerebral injuries, but the main barriers are to obtain hMSCs at sufficient quantity with required potency and to enhance survival and function upon transplantation [Sotiropoulou et al., 2006; Prockop et al., 2010]. Strategies from addition of soluble growth factors to materials surface engineering or hypoxia pretreatment have been actively sought to maintain hMSC therapeutic potency during expansion and to improve the survival of the transplanted cells [Hu et al., 2008; Hudalla et al., 2011]. MSCs are significant source of endogenous growth factors and ECM proteins that influence hMSC fate via paracrine and autocrine actions [Parekkadan and Milwid, 2010; Prockop et al., 2010]. Among various endogenous growth factors, FGF-2, a pluripotent cytokine, promotes hMSC proliferation while preserving multipotentiality and has been commonly used as a culture supplement in hMSC expansion including clinical trials [Sensebe et al., 2010]. Autocrine FGF signaling has also been shown to influence hMSC properties in culture [Zaragosi et al., 2006; Rider et al., 2008]. On the other hand, MSC-derived ECM matrices improved hMSC multi-lineage potential and resistance to oxidative stress, partially due to their capacity to bind with growth factors [Chen et al., 2007; Lai et al., 2010; Pei et al., 2011]. FGF-2 is known to interact with the components of the ECM network such as glycosaminoglycans (GAGs) and proteoglycans

Conflict of interest: none to declare.

Grant sponsor: The American Heart Association Grant-in-Aid; Grant number: 10GRNT3860040; Grant sponsor: DOD Peer Reviewed Medical Research Program; Grant number: W81XWH-07-1-0363.

*Correspondence to: Teng Ma, PhD, Department of Chemical and Biomedical Engineering, Florida State University, 2525 Pottsdamer Street, Tallahassee, FL 32310. E-mail: teng@eng.fsu.edu

Manuscript Received: 11 July 2012; Manuscript Accepted: 26 September 2012

Accepted manuscript online in Wiley Online Library (wileyonlinelibrary.com): 11 October 2012

DOI 10.1002/jcb.24413 • © 2012 Wiley Periodicals, Inc.

(PGs) [Moscatelli, 1992; Fannon et al., 2000], but the impact of such interactions on hMSC properties remains unknown.

Bone marrow-derived hMSCs reside in their specialized niche characterized by a hypoxic microenvironment and by their intimate interactions with a network of ECM proteins [Ma et al., 2009]. ECM proteins not only provide the well-known structural support but also are being recognized as localized signal integrators through which growth factor binding, sequestration, subsequent activation, and release are regulated [Hynes, 2009]. Individual ECM components, including collagen-1 (COL I), vitronectin (VN), fibronectin (FN), and laminin (LN), have been tested to preserve hMSC properties [Klees et al., 2005; Salasznyk et al., 2007]. However, it has been suggested that individual ECM components are inadequate to mimic the complexity of the endogenous ECM and to direct specific, complex cell behaviors [Carson and Barker, 2009]. Using the ECM matrices derived from cell culture, studies have shown that the MSC-derived ECM matrices significantly improved MSC proliferation without spontaneous differentiation and retained a stem cell population with lower level of reactive oxygen species (ROS) compared to the tissue culture plastics (TCP) coated with serum, FN or COL [Chen et al., 2007; Lai et al., 2010; Pei et al., 2011]. Other studies have also shown that the ECM matrices derived under different differentiation stages regulated hMSC fate in a stage-specific manner, suggesting the specificity of MSC extracellular milieu in directing MSC fate [Hoshiba et al., 2010].

Parallel to the effort to decipher the role of the ECM matrices in directing cell fate, it has been established that oxygen tension significantly influences hMSC properties. Oxygen tension in the conventional culture system is 20%, which is considerably higher than O_2 level in the bone marrow (about 1–2%) [Ivanovic, 2009; Ma et al., 2009]. Many studies have demonstrated that hypoxic culture preserved hMSC stemness with higher colony numbers and stem cell genes (e.g., OCT-4 and Rex-1) and regulated MSC proliferation, metabolism, mobilization, and homing [Annabi et al., 2003; D'Ippolito et al., 2004; Dos Santos et al., 2010]. Hypoxic condition also enhanced the secretion of endogenous growth factors [e.g., FGF-2, vascular endothelial growth factor (VEGF), and insulin-like growth factor (IGF)] and ECM proteins (e.g., COL I and FN) as well as the in vitro migration capacity of MSCs [Annabi et al., 2003; Grayson et al., 2006; Rosova et al., 2008]. While hypoxia-inducible factors (HIFs) are the master regulators for hMSC hypoxic responses [Grayson et al., 2007; Ohnishi et al., 2007; Liu et al., 2010], the role of hypoxia in regulating the hMSC extracellular milieu has not been fully understood.

Since both hypoxia and the ECM are integral components of hMSC microenvironment, we hypothesize that hypoxia influences hMSC properties in part through regulation of extracellular milieu characterized by the ECM matrices and the associated FGF-2. The results showed that the ECM matrices derived under different oxygen conditions differentially regulated their FGF-2-binding capacity and that autocrine FGF-2 signaling played an important role in mediating the hMSC–ECM interactions. The results highlight the interplay between the physiological and cellular components of the hMSC microenvironment and the need to integrate these components in hMSC expansion and transplantation.

MATERIALS AND METHODS

hMSCs

Standardized frozen hMSCs were obtained from the Tulane Center for Gene Therapy and cultured following the method outlined in our prior publications [Grayson et al., 2004; Zhao and Ma, 2005]. Briefly, hMSCs were expanded using minimum essential medium-alpha (α-MEM) (Life Technologies, Carlsbad, CA) supplemented with 1% Penicillin/Streptomycin (Life Technologies, MD) and 10% fetal bovine serum (FBS) (Atlanta Biologicals, Lawrenceville, GA) (growth media) in a standard CO_2 incubator (37°C and 5% CO_2). Cells from the same donor at passages 5–6 were seeded for each experiment and cells from multiple donors were used in experiments. All reagents were purchased from Sigma–Aldrich (St. Louis, MO) and all antibodies were purchased from Abcam (San Diego, CA) unless otherwise noted.

PREPARATION OF THE DECELLULARIZED ECM MATRICES

hMSCs were seeded in six-well plates containing a 22-mm diameter Thermanox plastic coverslip (Nalge Nunc International, Rochester, NY) at 1×10^5 cells/well in growth media. Cells were cultured under normoxia (20% O_2) in a standard CO_2 incubator or hypoxia (2% O_2) in a C-Chamber (BioSpherix, Lacona, NY) for up to 15 days. Media preconditioned under respective oxygen tension were changed every 3 days. Ascorbic acid (50 μM) was added during the final 8 days of culture. For decellularization, samples were first washed with phosphate-buffered saline (PBS) and then incubated with 0.5% Triton X-100 containing 20 mM NH_4OH in PBS for 10 min at 37°C, followed by the treatment with DNase (100 U/ml) for 1 h at 37°C [Chen et al., 2007]. The decellularized ECM matrices obtained from normoxic and hypoxic culture conditions were termed M(N) and M(H), respectively (Fig. 1). The plastic coverslips pre-coated with serum were used as controls and termed TCP.

IMMUNOSTAINING AND ENZYME-LINKED IMMUNOSORBENT ASSAY (ELISA)

Expression of ECM proteins was examined by immunocytochemistry staining as described previously [Grayson et al., 2004]. Briefly, the ECM matrices were fixed with 4% paraformaldehyde (PFA), permeabilized with 0.5% Triton X-100 in PBS, blocked with 1% bovine serum albumin (BSA) in PBS, and incubated with primary antibodies, followed by fluorescein isothiocyanate (FITC)-conjugated secondary antibody (Jackson Laboratories, West Grove, PA). The cell nuclei were counterstained with 4′,6-diamidino-2-phenylindole (DAPI), and visualized using an Olympus IX70 (Center Valley, PA) with an Optronics (Goleta, CA) camera attachment.

ECM proteins were quantified by in situ ELISA following a method outlined in one of our prior publications [Kim and Ma, 2012]. Briefly, samples were washed with PBS and fixed with 4% PFA in PBS for 1 h. After PBS wash, the samples were permeablized by washing with 0.2–0.5% Triton X-100 in PBS twice and then incubated with blocking buffer, 1% BSA in PBS, for 30 min. Samples were incubated with primary antibody overnight at 4°C, washed with blocking buffer, and incubated with an alkaline phosphatase (ALP)-conjugated secondary antibody for 1 h at the room temperature. After blocking buffer wash, 1 ml para-nitrophenolphosphate

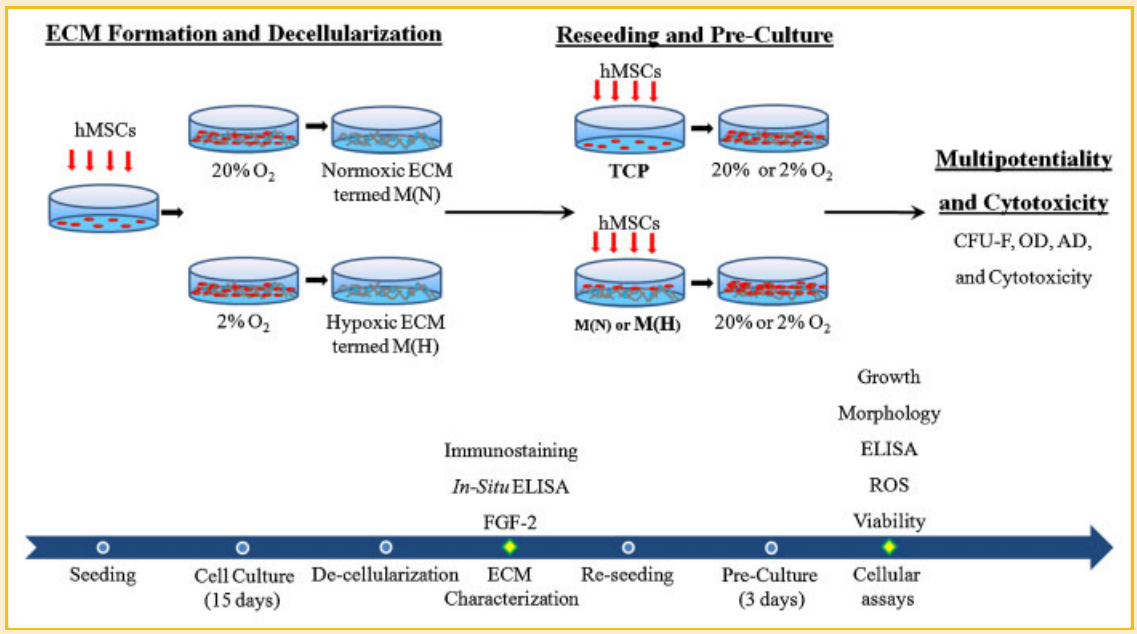

Fig. 1. The schematics of the experimental design. ECM matrices were formed by de-cellularization processes after 15 days of culture under standard and hypoxic culture conditions, respectively. After decellularization, the morphology of the ECM matrices was characterized by immunostaining and expression of ECM proteins and FGF-2 were quantified by ELISA. To evaluate cellular responses, hMSCs were then re-seeded on the decellularized ECM matrices and cell responses were evaluated after 3 days of culture under two oxygen tensions. The cells on the ECM matrices were also induced to undergo adipogenic and osteogenic differentiation for 5 and 20 days, respectively.

(PNPP) substrate was added to samples and incubated at 37°C for 15 min. After the addition of 0.5 N NaOH stop solution, the absorbance was spectrophotometrically measured at a wavelength of 405 nm and background absorbance at 655 nm was subtracted.

MEASUREMENT OF FGF-2

Normoxic- and hypoxic-conditioned media were collected when hMSCs were cultured with serum-free media under normoxia and hypoxia for 24 h, respectively. Matrix-bound FGF-2 was extracted from the decellularized ECM matrices by the treatment with 2 M NaCl (pH 7.4) solution following a method by Fannon et al. [2000]. Same procedure was also used to extract FGF-2 from hMSCs reseeded on the TCP or the decellularized ECM matrices after 3 days of culture. The extracted FGF-2 and free FGF-2 in media were quantified using a FGF-2 ELISA Assay Kit (R&D systems, Minneapolis, MN). FGF-2 protein was purchased from R&D systems.

DNA ASSAYS, CELL VIABILITY, AND COLONY-FORMING UNIT-FIBROBLASTIC (CFU-F)

DNA assay was used to quantify cell number on the TCP or the ECM matrices following a method reported in one of our previous publications [Zhao and Ma, 2005]. Briefly, cells were lysed using a Tris-EDTA-Triton-X 100 (TEX) solution with proteinase K at 50°C overnight. Picogreen (Molecular Probes, Eugene, OR) was added to triplicate samples and a series of DNA standards in a 96-well plate, which was then incubated and read using Fluoro Count (PerkinElmer, Boston, MA). hMSCs were found to contain an average of 9.3 pg DNA/cell in one of our prior studies [Zhao and Ma, 2005], which was used to convert DNA concentration to cell number. For cell number, triplicate samples from each condition were used for each data point, and three independent runs were repeated under identical operation conditions. For FGF-2 inhibition studies, hMSCs were seeded at 1,000 cells per cm^2 and cultured for 6 days in the presence of SU5402 [10 μM in dimethyl sulfoxide (DMSO)], a FGFR1 inhibitor (Calbiochem, San Diego, CA), while DMSO alone was used as control. Cell viability was measured by thiazolyl blue tetrazolium bromide (MTT) assay as outlined in one of [Sellgren and Ma, 2012]. For ERK activity in the presence of MEK inhibitor, U-0126 (Enzo Life Sciences International, Farmingdale, NY), hMSCs were seeded at 1.0×10^4 cells/cm^2 and cultured for 24 h in the presence of U-0126 at 20.0 μM and DMSO alone as control for all substrates. Phosphorylated ERK (pERK) was measured by an ELISA assay kit (Enzo Life Sciences International) and normalized to cell number.

CFU-F numbers were determined following a method reported in one of our previous publications [Zhao et al., 2009]. Briefly, the cells were harvested from the decellularized matrices and the TCP using PBS containing 0.5% trypsin/0.25% collagenase/1 mM EDTA. After cell counting, hMSCs were seeded at 10 cells per cm^2. After 14 days of culture, cells were washed with PBS and stained with 0.5% crystal violet solution for 15 min at room temperature. After washing with PBS three times, the colonies were counted manually. The colony number was the average of colonies from three samples for each condition.

OSTEOGENIC DIFFERENTIATION

After 3 days of culture on the decellularized matrices and the TCP under two different oxygen tensions, the growth media were

replaced with the osteogenic media (high glucose Dulbecco's modified eagle medium (DMEM) (Life Technologies, Carlsbad, CA) supplemented with 10% FBS, 1% penicillin/streptomycin, 100 nM dexamethasone, 10 nM sodium-β-glycerophosphate, and 12.8 mg/L ascorbic acid-2 phosphate) for an additional 5 days following the previously reported method [Grayson et al., 2004]. After 5 days of culture in the differentiation media, calcium mineralization was quantified and stained by Alizarin Red S and von Kossa, respectively. Briefly, the samples were washed with PBS, fixed in 4% PFA solution for 1 h, and then washed with DI-water. For the quantification of calcium deposition, the samples were stained with Alizarin Red S. After washing with DI water, calcium was desorbed in 10% cetylpyridinium chloride (CPS). The absorbance was spectrophotometrically measured at a wavelength of 540 nm and normalized to cell number. For von Kossa staining, the samples were incubated in 5% silver nitrate solution under a UV light for approximately 30 min, washed in 5% sodium thiosulfate solution for 5 min, and stained with 0.1% nuclear fast red solution for 3 min. After DI-water wash, the samples were viewed using an Olympus IX70 with an Optronics camera attachment.

ADIPOGENIC DIFFERENTIATION

After 3 days of culture on the ECM matrices and the TCP under two oxygen conditions, the growth media were replaced with the adipogenic induction and maintenance media following a previously reported method [Grayson et al., 2004]. Briefly, the samples were induced by treating with adipogenic induction (AI) medium (high-glucose DMEM supplemented with 10% FBS, 1% Penicillin/Streptomycin, 0.2 mM indomethacin, 0.5 mM isobutyl-1-methyl xanthine, 1 μM dexamethasone, and 10 μg/ml insulin). After 2 days, the AI media was removed and replaced with adipogenic maintenance (AM) medium (high-glucose DMEM supplemented with 10% FBS, 1% Penicillin/Streptomycin, and 10 μg/ml insulin) for another 2 days. This treatment was continued in a cyclic fashion for 20 days. Differentiation into adipocytes was quantified and visualized by Oil Red O staining of the lipid vacuoles. Briefly, the samples were fixed in 4% PFA for 1 h, washed with DI-water, and washed with 60% *iso*-propanol. After the incubation in Oil Red O solution for 5 min, the samples were washed and viewed using an Olympus IX70 with an Optronics camera attachment. For the quantification of lipid droplets, the dye retained by the cells was eluted by *iso*-propanol and the absorbance was spectrophotometrically measured at a wavelength of 540 nm and normalized to cell number.

MEASUREMENTS OF INTRACELLULAR ROS

Intracellular ROS was measured with carboxy-H_2DCFDA using a ROS Detection Kit (Invitrogen, Eugene, OR) following the manufacturer's instruction. Briefly, hMSCs were seeded on the ECM matrices and the TCP in growth media. After 3 days of culture, ROS positive cells were counted with or without the treatment of *tert*-butyl hydroperoxide (TBHP), which is a common inducer of ROS production as a positive control. ROS levels were expressed as the percentage of ROS positive cells.

CELL VIABILITY AND CYTOTOXICITY

To determine cell viability in low serum, hMSCs were seeded on the ECM matrices and the TCP at 1,000 cells/well in growth media. After 24 h of incubation, the media were replaced with low serum growth media with 2% FBS and then incubated under hypoxia or normoxia for an additional 6 days. Cell viability was determined by MTT assay. For the cytotoxicity assay, hMSCs were seeded on the ECM matrices and the TCP under two different oxygen tensions and cultured for up to 3 days. After culturing for 3 days, cells were placed in serum-free media for an additional 24 h. Lactate dehydrogenase (LDH) was measured by a Cytotoxicity Detection Kit (Roche Diagnostics Corporation, Indianapolis, IN).

STATISTICS/DATA ANALYSIS

At least triplicate experiments were performed and the representative results were reported. All data points were an average of at least three replicates and expressed as means ± standard deviation of the means of samples. Statistical comparisons were performed by ANOVA for multiple comparisons and statistical significance was accepted at $P < 0.05$.

RESULTS

CHARACTERISTICS OF HMSC-DERIVED ECM MATRICES AND MATRIX-BOUND FGF-2

On the decellularized ECM matrices, the structures of the major ECM proteins, including FN, LN, VN, COL-I, and COL-IV, were maintained (Fig. 2A). However, quantitative analysis of ECM proteins revealed the major differences during the initial culture period and after cell removal under two different oxygen tensions (Fig. 2B). In the first week of culture, FN (1.4 times) and COL I (1.2 times) were significantly higher under hypoxia as compared to their normoxic counterparts (Fig. 2B(i,ii)). Similar trends were observed for COL IV, VN, and LN. After cell removal at day 15, COL I in the M(H) remained 1.7 times higher than that of the M(N), but COL IV and LN in the M(N) were 1.9 and 3.9 times higher than those of the M(H) (Fig. 2B(iii)). FN and VN expressions were comparable in the ECM matrices.

Matrix-bound FGF-2 measured by ELISA was used to determine the retention of endogenous FGF-2 after cell removal. Matrix-bound FGF-2 was released from the decellularized matrices by a brief treatment with 2.0 M NaCl (pH 7.4) solution following the method by Fannon et al. [2000]. Matrix-bound FGF-2 on the M(H) was 1.7 times higher than that on the M(N) immediately after cell removal (Fig. 3A) but declined to undetectable level after 24 h. To examine the FGF-2 adsorption capacity of the decellularized ECM matrices, conditioned media obtained under normoxic (N-CM) or hypoxic (H-CM) condition were added to the decellularized ECM matrices 24-h post-decellularization when the residual FGF-2 on the matrices was undetectable. Despite the lower levels compared to the freshly decelluarized ECM matrices, matrix-bound FGF-2 on the M(H) was higher than that on the M(N) for the conditioned media from both oxygen tensions. To further examine FGF-2 binding capacity, exogenous FGF-2 at 10 ng/ml was added to the decellularized ECM matrices for 24-h post-decellularization and matrix-bound FGF-2 on the M(H) was 2.9 times higher compared to that on the M(N).

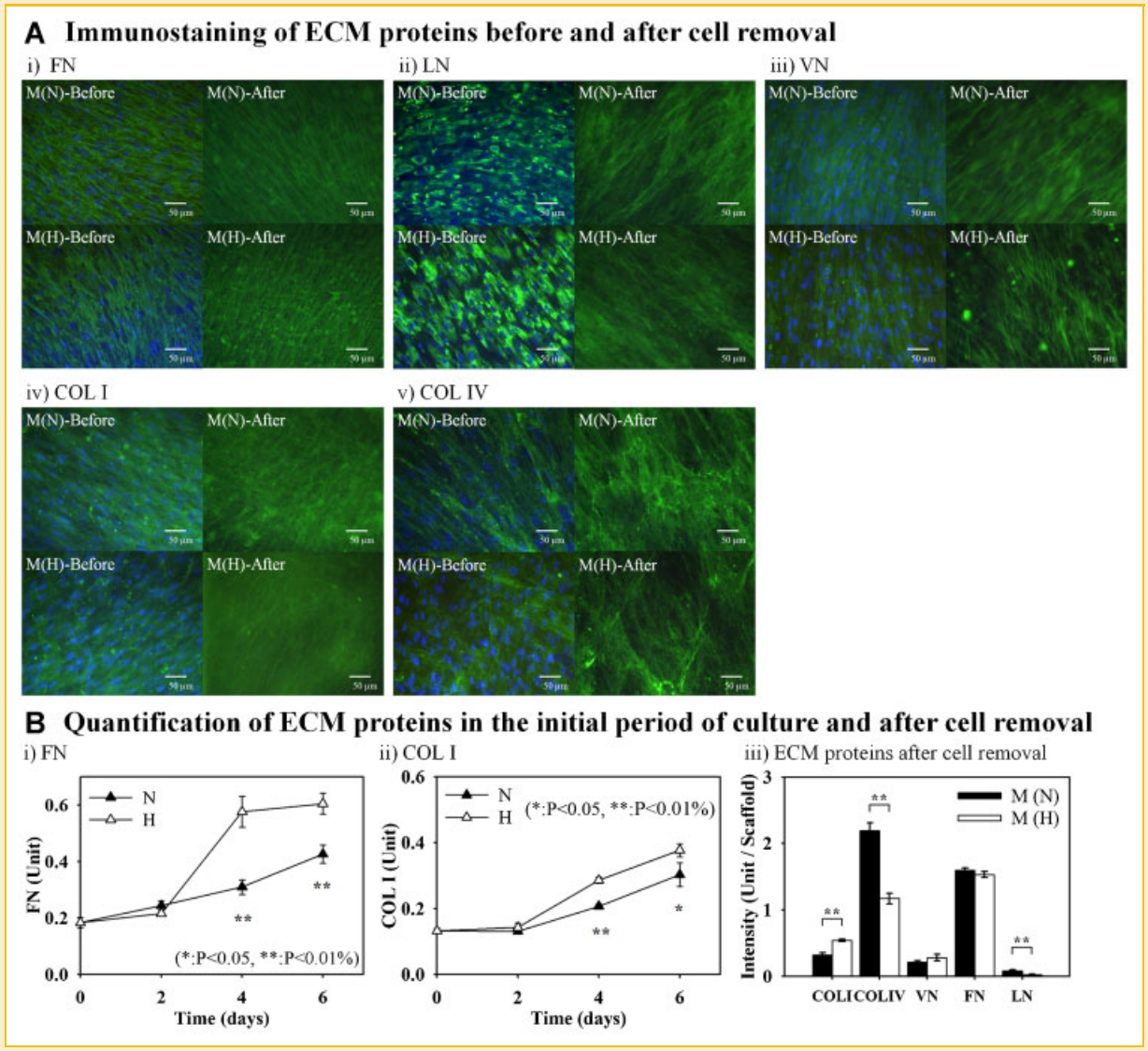

Fig. 2. Characteristics of hMSC-derived ECM under two oxygen tensions. A: Components of hMSC-derived ECM were visualized by immunostaining before and after cell removal. Blue and green represent cell nuclei and the ECM components, respectively. B: Quantification of ECM proteins. In the initial period, cells under hypoxia secreted more extensive FN and Col I compared to their normoxia counterparts (B(i,ii)). After cell removal at Day 15, the expression of COL I in the M(H) remained higher than those of the M(N). However, COL IV and LN in the M(N) were higher than those of the M(H), while FN and VN expressions were comparable in the decellularized ECM matrices after cell removal (B(iii)). Values are expressed as means ± SD of three samples of each condition ($^{*}P < 0.05$, $^{**}P < 0.01$). Magnification: 200×.

AUTOCRINE FGF-2 SECRETION ON THE DECELLULARIZED ECM MATRICES

To interrogate the reciprocal interactions between autocrine FGF-2 and ECM matrices, hMSCs were re-seeded on the ECM matrices and free and matrix-bound FGF-2 were determined after 3 days of culture under normoxia (Fig. 3B,C). The 3-day culture period was chosen to minimize the influence of the newly synthesized ECM matrices while ensuring cell adhesion and endogenous FGF-2 secretion. Free FGF-2 secretion was two times higher on the M(H) compared to the M(N) with both significantly higher than the TCP, suggesting the stimulatory effects of the ECM matrices on endogenous FGF-2 secretion. For the matrix-bound FGF-2, the M(H) had the highest secretion while the M(N) and the TCP are comparable. For total FGF-2 secretion, the M(H) was 1.69 and 2.85 times higher than that of the M(N) and the TCP, respectively.

ACTIVATION OF ERK1/2 PATHWAYS

To identify the pathways involved in the ECM matrix-mediated effects on hMSC proliferation and multi-lineage differentiation, pERK1/2 expression was measured by ELISA. hMSCs on the M(H) had significantly higher pERK1/2 expression 24 h after reseeding compared to the M(N), with the TCP having the lowest expression (Fig. 3E). The addition of the MEK inhibitor (U-0126) significantly decreased ERK activity (about 30% decreases) on all substrates under both normoxia and hypoxia.

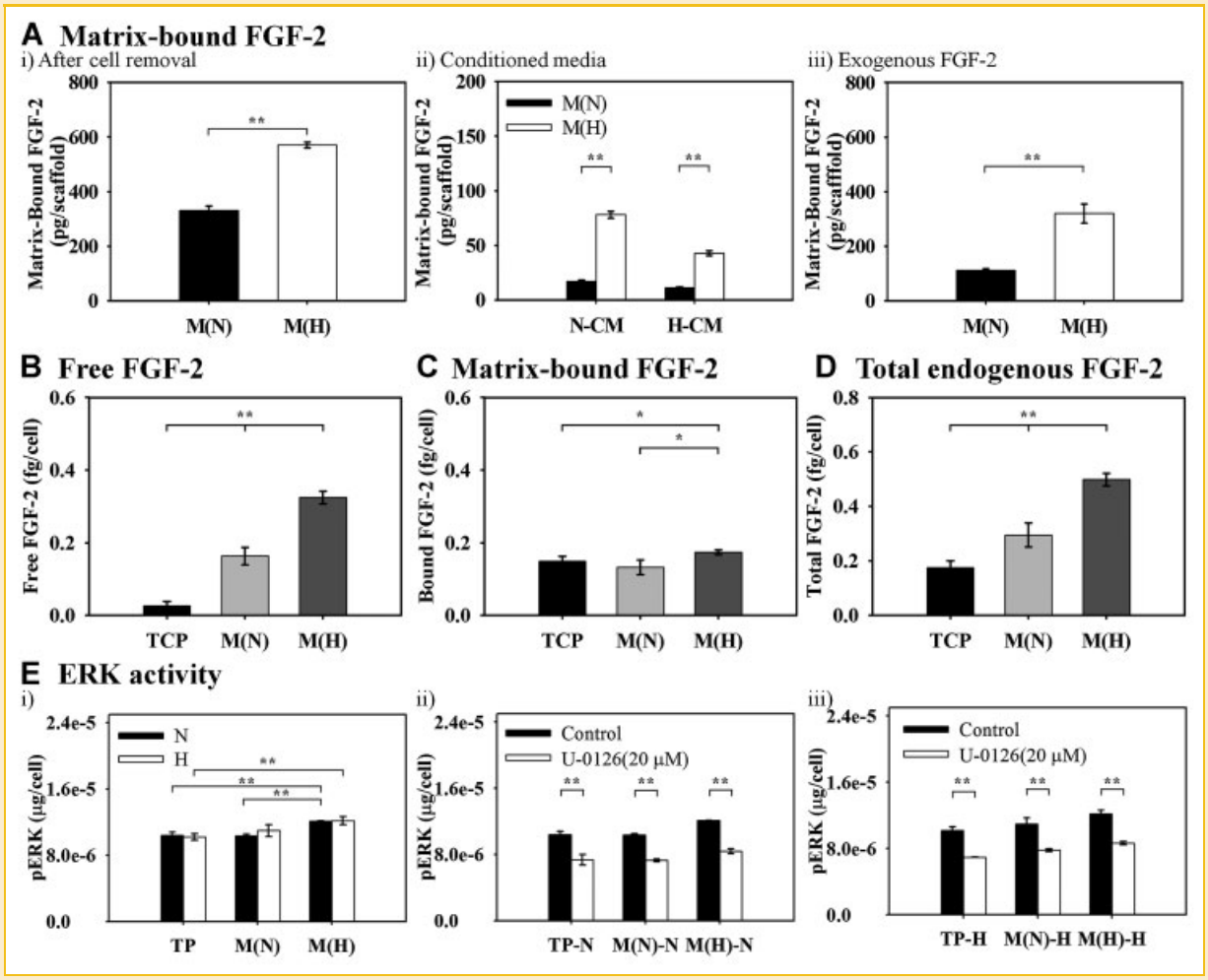

Fig. 3. Free and Matrix-bound FGF-2 and ERK activation. A: Matrix-bound FGF-2 immediately after cell removal. Matrix-bound FGF-2 after cell removal was significantly higher in the M(H) compared to that on the M(N). Similar trends were observed with the treatment of normoxic- and hypoxic-conditioned media and 10 ng exogenous FGF-2. B–D: Three days after reseeding and normoxia culture, free, matrix-bound, and total endogenous FGF-2 was the highest in the M(H) among three substrates. E: Adhesion to the M(H) significantly enhanced pERK expression. Addition of U-0126 significantly reduced pERK expression for all three substrates obtained under two oxygen conditions. Values are expressed as means ± SD of three samples of each condition ($^{*}P < 0.05$, $^{**}P < 0.01$).

CELL PROLIFERATION AND CFU-F

Cell numbers on the M(N) and the M(H) under normoxia were significantly higher (1.2 and 1.3 times, respectively) than those on the TCP at day 1, but hypoxic condition had minimal effects on all substrates (Fig. 4A). After 3 days of culture, cell number on the M(N) and the M(H) increased 4.3 and 4.6 times, respectively, compared to 2.9 times increase on the TCP. Hypoxic culture condition further enhanced hMSC proliferation with 33%, 13%, and 15% increases after 3 days of culture on the TCP, the M(N), and the M(H), respectively. To investigate if autocrine FGF-2 influences cell proliferation, hMSCs at passage 4 and 6 were cultured on the decellularized ECM matrices and the TCP for 6 days in the presence of SU5402 and DMSO carrier alone as controls. For both passages, the addition of SU5402 resulted in reduction of cell number at 46.4%, 42.2%, and 40.9% of the respective DMSO carrier controls for the TCP, the M(N), and the M(H), respectively (Fig. 4B). Cell morphology revealed by F-actin staining was dramatically different between the TCP and the decellularized ECM matrices (Fig. 4C); cells on the TCP were flat and large, while the ECM matrices maintained the spindle shape.

The proportion of primitive hMSCs after 3 days of expansion on the ECM matrices was determined by CFU-F numbers (Fig. 4D, E). While both the M(H) and the M(N) had higher CFU-F than the TCP, CFU-F number on the M(H) was 1.18 times higher than that on the M(N), suggesting M(H)'s enhanced capacity in preserving CFU-F forming capacity compared to the M(N). Hypoxia further increased CFU-F numbers compared to normoxia for all three substrates at 47%, 19%, and 13% for the TCP, the M(N), and the M(H), respectively.

OSTEOGENIC AND ADIPOGENIC DIFFERENTIATION POTENTIALS

After reseeding and 3 days of culture in growth media under two oxygen tensions, hMSCs on the decellularized ECM matrices and the TCP were induced to undergo osteogenic and adipogenic differentiation under standard induction condition (e.g., normoxia in 5% CO_2 incubator) (Fig. 5). After 5 days of incubation in the OI media, hMSCs

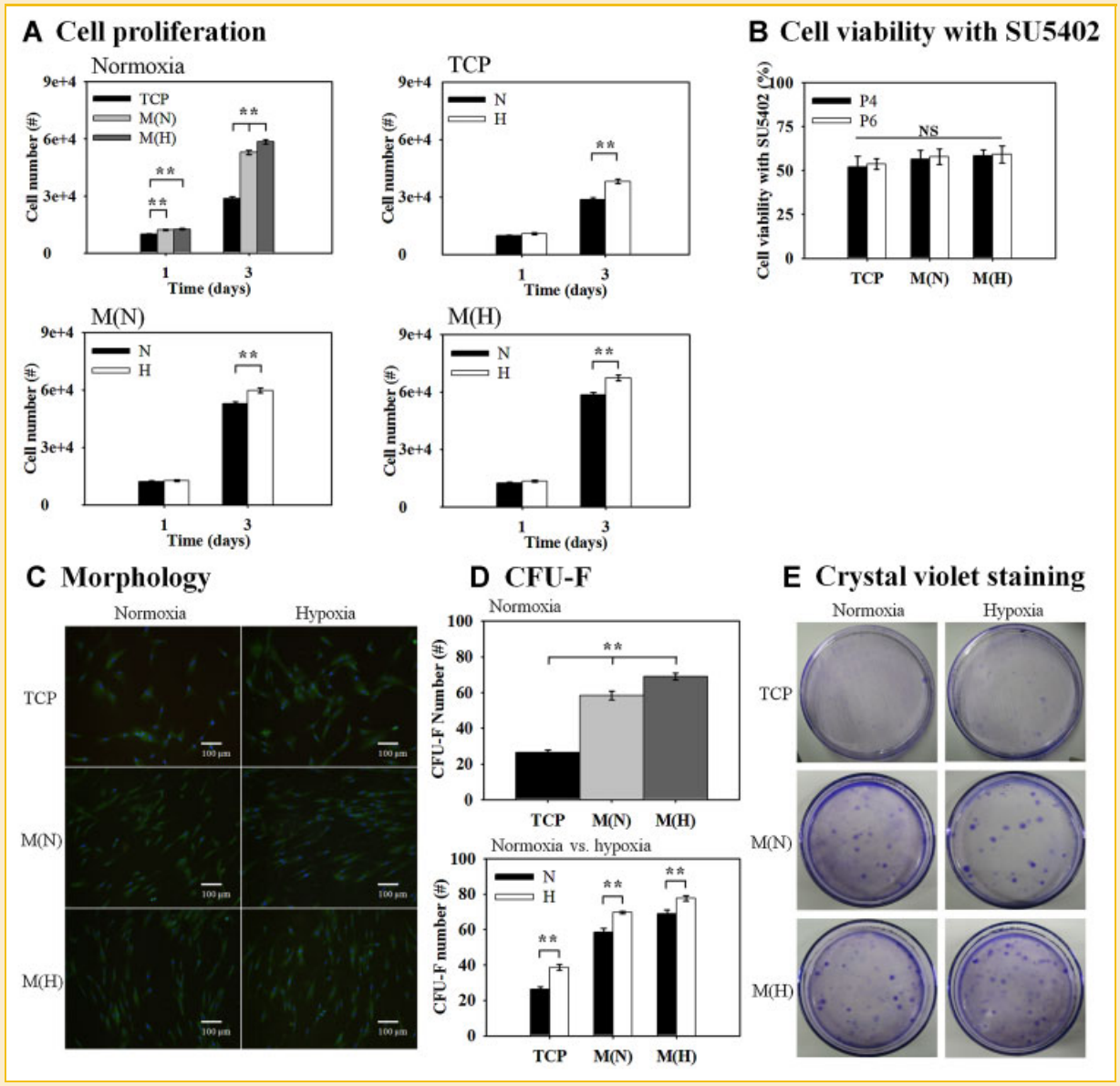

Fig. 4. hMSC growth and CFU-F formation on the decellularized ECM matrices after 3 days of culture under two oxygen tensions. A: Cell proliferation was significantly enhanced on the M(N) and the M(H) compared to the TCP. Hypoxia further increased cell proliferation on all substrates. B: Addition of FGF-2 inhibitor SU5402 for p4 and p6 hMSCs reduced cell number to comparable levels on all three substrates. C: F-actin staining revealed small and spindle-shaped hMSCs on the M(H) and the M(N) compared to the large and flat cells on the TCP. D,E: CFU-F numbers had similar trends as the cell growth with the highest CFU-F expression on the M(H). Hypoxia enhanced CFU-F expression on all three substrates. Colony sizes on the M(N) and the M(H) were also much bigger than ones on the TCP. Values are expressed as means ± SD of three samples of each condition ($^{*}P < 0.05$, $^{**}P < 0.01$). Magnification: 100×.

on the M(H) exhibited increased calcium depositions compared to those on the M(N), while both the M(H) and the M(N) had higher calcium deposition than the TCP (1.5 and 1.9 times, respectively) (Fig. 5A). The hypoxic culture in growth media further enhanced the calcium deposition on the TCP and the M(N) (1.5 and 1.1 times, respectively), but not on the M(H). After 20 days of adipogenic differentiation, the intensity of hMSC adipogenic differentiation on the M(H) was significantly higher than that on the M(N), while 3 days of hypoxic culture in growth media further enhanced Oil Red O expression on the TCP and the M(N) (1.5 and 1.4 times, respectively), but not on the M(H) (Fig. 5B).

INTRACELLULAR ROS WITH OR WITHOUT TBHP TREATMENT

About half of cells cultured on the TCP under normoxia were intracellular ROS positive, while only 14% of cells on the TCP under hypoxia were ROS positive (Fig. 6A). In contrast, cells on both the M(N) and the M(H) were ROS negative under both oxygen conditions. The TBHP treatment significantly increased the percentage of ROS positive cells, resulting in 92%, 74%, and 67% of ROS-positive cells on the TCP, the M(N), and the M(H), respectively. However, there was no difference in the percentage of ROS expressing cells between the M(N) and the M(H) under two oxygen tensions post-TBHP treatment (data not shown).

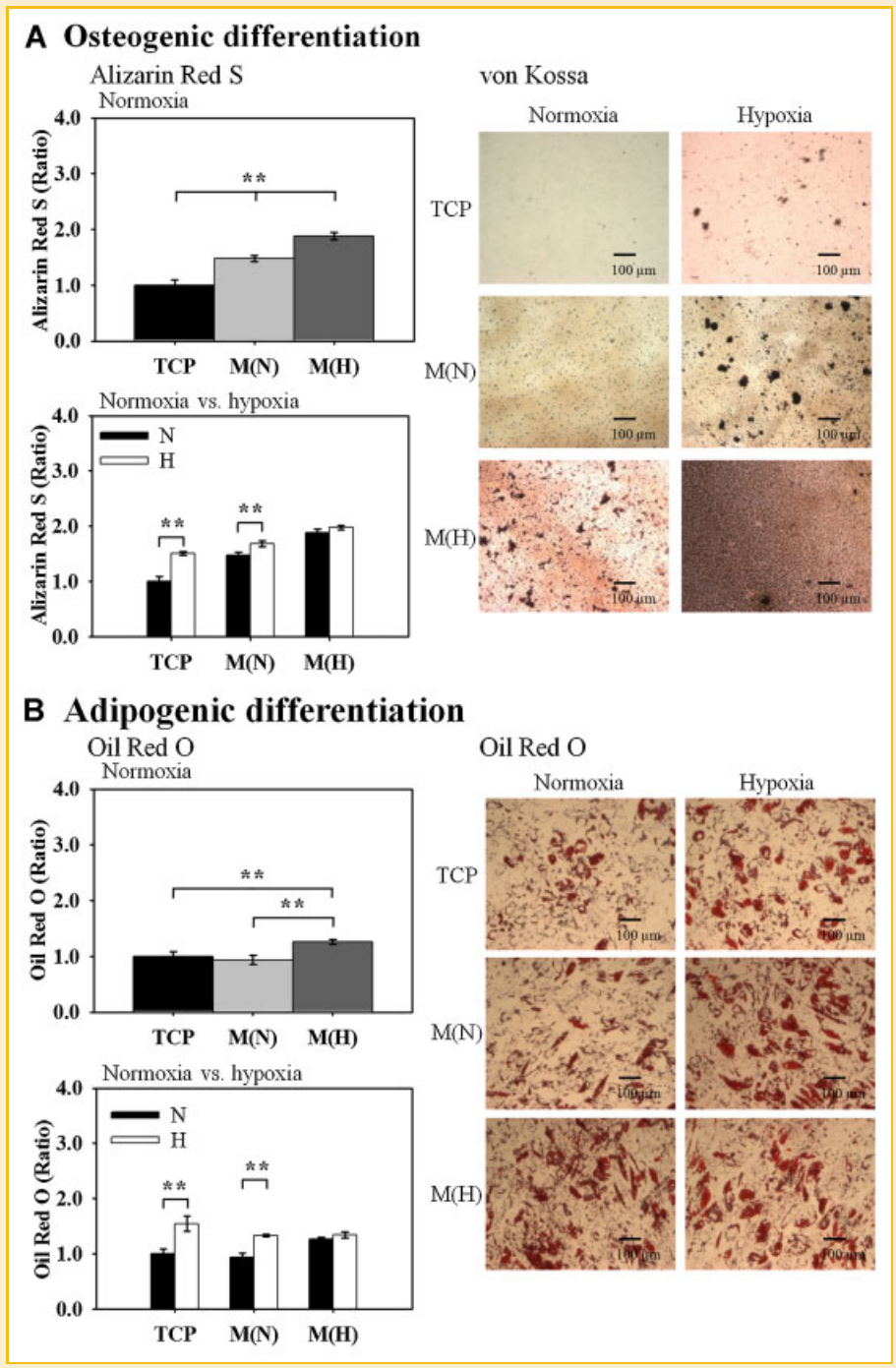

Fig. 5. Osteogenic and adipogenic differentiation on the decellularized ECM matrices. After reseeding on the ECM matrices and 3 days of culture, hMSCs were induced to undergo osteogenic and adipogenic differentiation, respectively. A: After 5 days of osteogenic induction, significant calcium deposition was displayed on the M(H) and the M(N) as indicated by von Kossa staining. Three days of pre-culture under hypoxia further enhanced mineralization on the M(N) but not the M(H). B: After 20 days of adipogenic induction, intensity of Oil Red O expression was the highest in the M(H) but hypoxia enhanced its expression on the M(N). Values are expressed as means ± SD of three samples of each condition ($^{*}P < 0.05$, $^{**}P < 0.01$). Magnification: 100×.

CELL VIABILITY AND CYTOTOXICITY UNDER SERUM WITHDRAWAL

To test the impact of the ECM matrices on hMSC proliferation under low serum and viability under serum deprivation, hMSCs were cultured on the decellularized ECM matrices and the TCP in low serum (2% FBS) for 7 days or serum-free media for 24 h, respectively. Under normoxia, attachment to the ECM matrices modestly improved hMSC viability with 1.2 and 1.5 times higher cell number on the M(N) and the M(H) compared to that on the TCP at day 7, respectively (Fig. 6B). In contrast, the combination of attachment to the ECM matrices and hypoxic culture dramatically

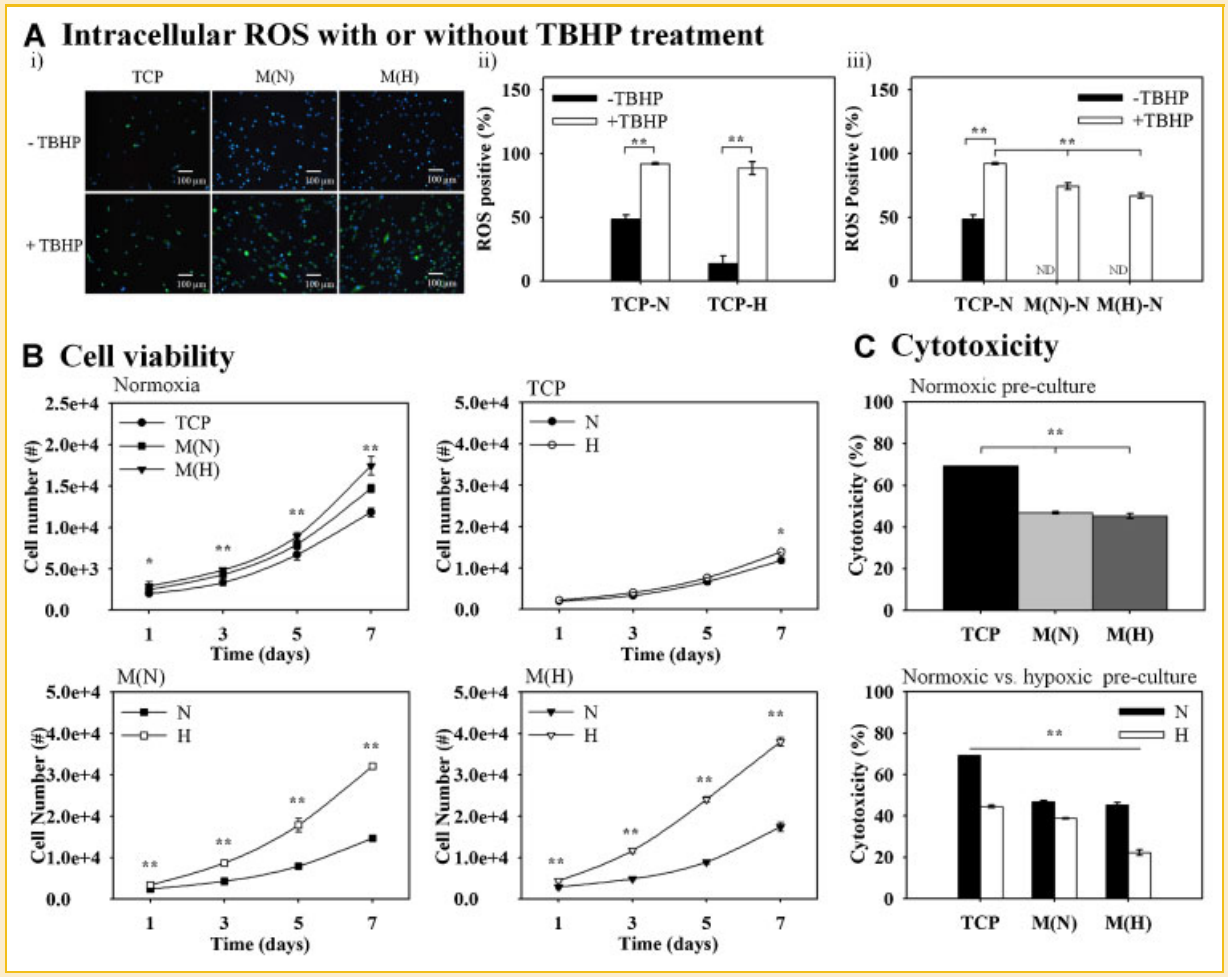

Fig. 6. Intracellular ROS, cell viability, and cytotoxicity under serum withdrawal after reseeding on the ECM matrices. A: Hypoxia culture reduced ROS expression on the TCP but addition of TBHP increased ROS to comparable levels. hMSCs cultured on the TCP had significantly higher ROS-positive cells compared to the negligible expression on both the M(N) and the M(H). The decellularized ECM matrices also significantly reduced ROS expression in the presence of TBHP. B: In media containing 2% serum, cell viability on the M(N) and the M(H) was significantly higher than that on the TCP under normoxia. However, hypoxia significantly increased cell viability on the M(N) and the M(H) with minimal impact on the TCP. C: In serum-free media, the ECM matrices and hypoxia significantly reduced the expression of LDH. Values are expressed as means ± SD of three samples of each condition ($^{*}P < 0.05$, $^{**}P < 0.01$). Magnification: 100×.

enhanced hMSC viability with 2.2 times higher cell number on both the M(N) and the M(H) at Day 7 compared to their normoxic counterparts. Attachment to the ECM matrices also resulted in lower levels of LDH with 69% on the TCP, 47% on the M(N), and 45% on the M(H), respectively. Culture in hypoxia further reduced the secretion of LDH for all three substrates (Fig. 6C).

DISCUSSION

HYPOXIA REGULATES ECM MICROENVIRONMENT: ECM PROTEINS AND FGF-2

Hypoxia stimulated the secretion of ECM proteins during the initial culture period with the most pronounced increases for FN, COL I, and LN, in agreement with the prior studies [Grayson et al., 2006; Zhao et al., 2010]. After 14 days of culture, however, the expression of FN and VN reached comparable levels under two oxygen conditions, suggesting the dynamic nature of the ECM composition as a combined result of secretion, sequestration, and proteolytic modification. The minimal structural changes of the ECM matrices revealed by immunostaining before and after cell removal indicated the maintenance of the ECM structure post-decellularization.

Oxygen tension is a developmentally important stimulus that regulates intrinsic stem cell properties including proliferation, multi-potentiality, and secretion of cytokines such as FGF-2, VEGF, transforming growth factor-β (TGF-β), and platelet-derived growth factor-β (PDGF-β) via HIF activation [Crisostomo et al., 2008; Rosova et al., 2008; Ivanovic, 2009]. Among these growth factors, the impact of autocrine FGF-2 on hMSC properties is well-documented, but its role in mediating cell-ECM interactions has not been reported [Bianchi et al., 2003; Zaragosi et al., 2006; Rider et al., 2008; Auletta et al., 2011]. In the current study, the residue FGF-2 in the decellularized ECM matrices was undetectable by ELISA 24-h post-decellularization, possibly due to the short half life on the decellularized ECM matrices [Moscatelli, 1992]. Because the total

ECM protein was not an accurate measurement of FGF-2 binding sites and the residual heparan sulfate proteoglycans (HSPGs) in the decellularized ECM matrices only represented a fraction of FGF-2 binding sites [Fannon et al., 2000] and were undetectable in our current study, the identification of the specific ECM components responsible for FGF-2 binding requires further study. However, the ECM matrices obtained under two oxygen tensions displayed differential binding capacities with exogenous FGF-2 and FGF-2 in the conditioned media (Fig. 3A). Furthermore, following reseeding onto the decellularized matrices, hMSCs also significantly increased FGF-2 secretion on the M(N) and the M(H), suggesting the stimulatory effects of ECM binding on the endogenous FGF-2 secretion with the M(H) having the highest potency. Similar to hypoxia culture, the enhanced endogenous FGF-2 secretion on the decellularized ECM matrices may be due to their ability to maintain hMSCs in a more primitive and proliferative state, which has shown to enhance endogenous FGF-2 secretion [Zaragosi et al., 2006].

Extracellular signal-related kinase (ERK) is a member of the mitogen-activated protein kinase (MAPK) family and its roles in regulating hMSC proliferation and lineage-specific differentiation have been well established [Carcamo-Orive et al., 2008; Choi et al., 2008; Lund et al., 2009]. ERK is indirectly activated by matrix adhesion and by mitogenic growth factors, such as FGF-2 and FGF-4, but the effects of hypoxia on ERK activation is controversial [Choi et al., 2008; Crisostomo et al., 2008; Jin et al., 2010]. Several studies have shown that hypoxic culture (e.g., 1% O_2) significantly increased pERK expression [Crisostomo et al., 2008; Wang et al., 2012], while Jin et al. [2010] reported decreases of pERK over long-term hypoxic hMSC expansion. In the current study, ERK activation was used as a discriminating point to interrogate the contribution of adhesion to the decellularized ECM matrices versus hypoxic culture condition. Hypoxic culture did not lead to significant variation in pERK expression on all three substrates, but adhesion to the M(H) resulted in significant increase in pERK expression. Thus, adhesion to the ECM matrices, at least to the M(H), was more potent in activating ERK compared to hypoxic culture. Indeed, addition of MEK inhibitor U-0126 after 24 h of culture reduced the pERK to basal levels in all culture conditions, confirming the role of ECM adhesion on ERK activation [Wang et al., 2012; Sharrocks, 2006]. Whether the ERK activation by hypoxia and/or by ECM adhesion differs in the temporal profile remains to be investigated.

HYPOXIA AND THE ECM MATRICES SYNERGISTICALLY PRESERVE hMSC PHENOTYPE

Population doubling time estimated on the M(H) and the M(N) under hypoxia were about 20 and 21 h, respectively, which were significantly lower than what was reported in hypoxic TCP culture (between 53 and 72 h) [Grayson et al., 2007; Jin et al., 2010] or the normoxic culture on the decellularized ECM matrices (about 41 h) [Pei et al., 2011]. The synergistic effects of hypoxia and the ECM matrices may be due to the local enrichment of endogenous FGF-2 stimulated by hypoxia. Indeed, addition of a FGF-2 inhibitor, SU5402, reduced hMSC proliferation to the basal level on all three substrates under both hypoxic and normoxic culture conditions, suggesting the autocrine FGF-2 effects as reported in prior studies [Zaragosi et al., 2006; Rider et al., 2008]. Zaragosi et al. [2006] revealed that human multipotent adiposed-derived stem (hMADS) cells in fast cycling secreted more FGF-2, resulting in much higher matrix-bound FGF-2 in the fast cycling cells as compared to that in the slow cycling cells. Thus, the pro-mitotic effects of endogenous FGF-2 under hypoxia were further propagated by the decellularized ECM matrices, serving as a localized reservoir.

The synergistic effects of hypoxia and the ECM matrices also enhanced CFU-F formation and multipotentiality. In addition to FGF-2, the decellularized ECM matrices enhanced MSC osteogenic and adipogenic differentiation compared to the TCP coated with components of ECM proteins [Chen et al., 2007; Lai et al., 2010]. Both the M(H) and the M(N) significantly enhanced hMSC osteogenic differentiation measured by Alizarin Red S and von Kossa staining, confirming previous findings [Chen et al., 2007]. For the adipogenic differentiation, only the M(H) had significantly higher Oil Red O expression compared to the TCP and the M(N), whereas hypoxic pre-culture enhanced the lipid formation on the TCP and the M(N). Pei et al. [2011] found that hMSCs expanded on the ECM matrices have decreased adipogenic capacity measured by Oil Red O but adipogenic induction was carried out after removing cells from the ECM matrices, which differed from our current study. Nonetheless, the enhanced osteogenic and adipogenic differentiation by the ECM matrices and hypoxia also appeared to be FGF-2-related, as reported in a prior study [Rider et al., 2008].

HYPOXIA AND HYPOXIC-ECM MATRIX PROTECT hMSCs FROM THE CELL DEATH UNDER THE STRESS

The poor survival and a lack of long-term engraftment due to the loss of matrix attachment and exposure to the harsh in vivo ischemic environment of low nutrients and high oxidative stress (OS) are major obstacles for hMSC application in ischemic injuries [Copland and Galipeau, 2011; Fraser, 2011]. Among these factors, ROS are detrimental to cell survival and significantly reduced cell adhesion and viability both in vitro and in the transplanted region of an infracted heart [Song et al., 2010]. MSC expansion under the standard culture condition is known to increase the ROS level and cell senescence, but attachment to the decellularized ECM matrices has been shown to reduce MSC intracellular ROS level [Sun et al., 2011]. Interestingly, the cell source for the culture-derived ECM matrices also influenced the cellular ROS level in that the ECM matrices derived from young mice (3- vs. 18-month-old mice) were more potent in reducing ROS level presumably due to the factors embedded in the ECM [Sun et al., 2011]. Though the mechanism remains to be determined, the results of our current extended these observation and further suggest that attachment to the ECM matrices was more potent in reducing ROS compared to hypoxia with the M(H) having the highest anti-oxidant capacity.

Nutrient deprivation is another hallmark of ischemic injury and contributes to cell death of the transplanted hMSCs [Parekkadan and Milwid, 2010; Copland and Galipeau, 2011]. Under normoxia culture, the significant reduction of hMSC proliferation under 2% serum on all three substrates suggests a strong dependence of hMSC proliferation on the exogenous growth factors in serum. Surprisingly, hypoxic culture on the decellularized ECM matrices effectively overcome nutrient deprivation and restored hMSC proliferation to a level comparable to the normoxic TCP culture

in 10% serum; this is in sharp contrast to the minimal improvement in cell growth under the hypoxic TCP culture. It is postulated that the hypoxia-enhanced endogenous growth factor secretion is augmented by the presence of the decellularized ECM matrices and together they form a protective environment that overcomes nutrient depletion and sustains hMSC proliferation in the ischemic environment.

CONCLUSIONS

The results of the study demonstrate the interplay between the extracellular macromolecular milieu and physiological oxygen tension in directing hMSC fate and the central role of autocrine FGF-2 in mediating hMSC interaction with the ECM matrices. The results suggest that the recreation of extracellular microenvironment may be an effective approach to promote hMSC proliferation and survival in vivo.

REFERENCES

Annabi B, Lee YT, Turcotte S, Naud E, Desrosiers RR, Champagne M, Eliopoulos N, Galipeau J, Beliveau R. 2003. Hypoxia promotes murine bone-marrow-derived stromal cell migration and tube formation. Stem Cells 21:337–347.

Auletta JJ, Zale EA, Welter JF, Solchaga LA. 2011. Fibroblast growth factor-2 enhances expansion of human bone marrow-derived mesenchymal stromal cells without diminishing their immunosuppressive potential. Stem Cells Int 2011:235176.

Bianchi G, Banfi A, Mastrogiacomo M, Notaro R, Luzzatto L, Cancedda R, Quarto R. 2003. Ex vivo enrichment of mesenchymal cell progenitors by fibroblast growth factor 2. Exp Cell Res 287:98–105.

Carcamo-Orive I, Tejados N, Delgado J, Gaztelumendi A, Otaegui D, Lang V, Trigueros C. 2008. ERK2 protein regulates the proliferation of human mesenchymal stem cells without affecting their mobilization and differentiation potential. Exp Cell Res 314:1777–1788.

Carson AE, Barker TH. 2009. Emerging concepts in engineering extracellular matrix variants for directing cell phenotype. Regenerative Med 4:593–600.

Chen XD, Dusevich V, Feng JQ, Manolagas SC, Jilka RL. 2007. Extracellular matrix made by bone marrow cells facilitates expansion of marrow-derived mesenchymal progenitor cells and prevents their differentiation into osteoblasts. J Bone Miner Res 22:1943–1956.

Choi SC, Kim SJ, Choi JH, Park CY, Shim WJ, Lim DS. 2008. Fibroblast growth factor-2 and-4 promote the proliferation of bone marrow mesenchymal stem cells by the activation of the PI3K-Akt and ERK1/2 signaling pathways. Stem Cells Dev 17:725–736.

Copland IB, Galipeau J. 2011. Death and inflammation following somatic cell transplantation. Semin Immunopathol 33:535–550.

Crisostomo PR, Wang Y, Markel TA, Wang M, Lahm T, Meldrum DR. 2008. Human mesenchymal stem cells stimulated by TNF-alpha, LPS, or hypoxia produce growth factors by an NF kappa B- but not JNK-dependent mechanism. Am J Physiol Cell Physiol 294:C675–C682.

D'Ippolito G, Diabira S, Howard GA, Menei P, Roos BA, Schiller PC. 2004. Marrow-isolated adult multilineage inducible (MIAMI) cells, a unique population of postnatal young and old human cells with extensive expansion and differentiation potential. J Cell Sci 117:2971–2981.

Dos Santos F, Andrade PZ, Boura JS, Abecasis MM, Da Silva CL, Cabral JMS. 2010. Ex vivo expansion of human mesenchymal stem cells: A more effective cell proliferation kinetics and metabolism under hypoxia. J Cell Physiol 223:27–35.

Fannon M, Forsten KE, Nugent MA. 2000. Potentiation and inhibition of bFGF binding by heparin: A model for regulation of cellular response. Biochemistry 39:1434–1445.

Fraser PA. 2011. The role of free radical generation in increasing cerebrovascular permeability. Free Radic Biol Med 51:967–977.

Grayson WL, Ma T, Bunnell B. 2004. Human mesenchymal stem cells tissue development in 3D PET matrices. Biotechnol Prog 20:905–912.

Grayson WL, Zhao F, Bunnell B, Ma T. 2007. Hypoxia enhances proliferation and tissue formation of human mesenchymal stem cells. Biochem Biophys Res Commun 358:948–953.

Grayson WL, Zhao F, Izadpanah R, Bunnell B, Ma T. 2006. Effects of hypoxia on human mesenchymal stem cell expansion and plasticity in 3D constructs. J Cell Physiol 207:331–339.

Hoshiba T, Kawazoe N, Tateishi T, Chen GP. 2010. Development of extracellular matrices mimicking stepwise adipogenesis of mesenchymal stem cells. Adv Mater 22:3042–3047.

Hu XY, Yu SP, Fraser JL, Lu ZY, Ogle ME, Wang JA, Wei L. 2008. Transplantation of hypoxia-preconditioned mesenchymal stem cells improves infarcted heart function via enhanced survival of implanted cells and angiogenesis. J Thorac Cardiovasc Surg 135:799–808.

Hudalla GA, Kouris NA, Koepsel JT, Ogle BM, Murphy WL. 2011. Harnessing endogenous growth factor activity modulates stem cell behavior. Integr Biol 3:832–842.

Hynes RO. 2009. The extracellular matrix: Not just pretty fibrils. Science 326:1216–1219.

Ivanovic Z. 2009. Hypoxia or in situ normoxia: The stem coll paradigm. J Cell Physiol 219:271–275.

Jin YH, Kato T, Furu M, Nasu A, Kajita Y, Mitsui H, Ueda M, Aoyama T, Nakayama T, Nakamura T, Toguchida J. 2010. Mesenchymal stem cells cultured under hypoxia escape from senescence via down-regulation of p16 and extracellular signal regulated kinase. Biochem Biophys Res Commun 391:1471–1476.

Kim J, Ma T. 2012. Perfusion regulation of hMSC microenvironment and osteogenic differentiation in 3D scaffold. Biotechnol Bioeng 109:252–261.

Klees RF, Salasznyk RM, Kingsley K, Williams WA, Boskey A, Plopper GE. 2005. Laminin-5 induces osteogenic gene expression in human mesenchymal stem cells through an ERK-dependent pathway. Mol Biol Cell 16:881–890.

Lai YL, Sun Y, Skinner CM, Son EL, Lu ZD, Tuan RS, Jilka RL, Ling JA, Chen XD. 2010. Reconstitution of marrow-derived extracellular matrix ex vivo: A robust culture system for expanding large-scale highly functional human mesenchymal stem cells. Stem Cells Dev 19:1095–1107.

Liu HB, Xue WJ, Ge GQ, Luo XH, Li Y, Xiang HL, Ding XM, Tian PX, Tian XH. 2010. Hypoxic preconditioning advances CXCR4 and CXCR7 expression by activating HIF-1 alpha in MSCs. Biochem Biophys Res Commun 401:509–515.

Lund AW, Stegemann JP, Plopper GE. 2009. Inhibition of ERK promotes collagen gel compaction and fibrillogenesis to amplify the osteogenesis of human mesenchymal stem cells in three-dimensional collagen I culture. Stem Cells Dev 18:331–341.

Ma T, Grayson WL, Frohlich M, Vunjak-Novakovic G. 2009. Hypoxia and stem cell-based engineering of mesenchymal tissues. Biotechnol Prog 25:32–42.

Moscatelli D. 1992. Basic fibroblast growth-factor (bFGF) dissociates rapidly from heparan sulfates but slowly from receptors—Implications for mechanisms of bFGF release from pericellular matrix. J Biol Chem 267:25803–25809.

Ohnishi S, Yasuda T, Kitamura S, Nagaya N. 2007. Effect of hypoxia on gene expression of bone marrow-derived mesenchymal stem cells and mononuclear cells. Stem Cells 25:1166–1177.

Parekkadan B, Milwid JM. 2010. Mesenchymal stem cells as therapeutics. Ann Rev Biomed Eng 12(12):87–117.

Pei M, He F, Kish VL. 2011. Expansion on extracellular matrix deposited by human bone marrow stromal cells facilitates stem cell proliferation and tissue-specific lineage potential. Tissue Eng Part A 17:3067–3076.

Pittenger MF, Mackay AM, Beck SC, Jaiswal RK, Douglas R, Mosca JD, Moorman MA, Simonetti DW, Craig S, Marshak DR. 1999. Multilineage potential of adult human mesenchymal stem cells. Science 284:143–147.

Prockop DJ, Kota DJ, Bazhanov N, Reger RL. 2010. Evolving paradigms for repair of tissues by adult stem/progenitor cells (MSCs). J Cell Mol Med 14:2190–2199.

Rider DA, Dombrowski C, Sawyer AA, Ng GHB, Leong D, Hutmacher DW, Nurcombe V, Cool SM. 2008. Autocrine fibroblast growth factor 2 increases the multipotentiality of human adipose-derived mesenchymal stem cells. Stem Cells 26:1598–1608.

Rosova I, Dao M, Capoccia B, Link D, Nolta JA. 2008. Hypoxic preconditioning results in increased motility and improved therapeutic potential of human mesenchymal stem cells. Stem Cells 26:2173–2182.

Salasznyk RM, Klees RF, Williams WA, Boskey A, Plopper GE. 2007. Focal adhesion kinase signaling pathways regulate the osteogenic differentiation of human mesenchymal stem cells. Exp Cell Res 313:22–37.

Sellgren KL, Ma T. 2012. Perfusion conditioning of hydroxyapatite-chitosan-gelatin scaffolds for bone tissue regeneration from human mesenchymal stem cells. J Tissue Eng Regen Med 6:49–59.

Sensebe L, Krampera M, Schrezenmeier H, Bourin P, Giordano R. 2010. Mesenchymal stem cells for clinical application. Vox Sanguinis 98:93–107.

Sharrocks AD. 2006. Cell cycle: Sustained ERK signalling represses the inhibitors. Curr Biol 16:R540–R542.

Song H, Cha MJ, Song BW, Kim IK, Chang W, Lim S, Choi EJ, Ham O, Lee SY, Chung N, Jang Y, Hwang KC. 2010. Reactive oxygen species inhibit adhesion of mesenchymal stem cells implanted into ischemic myocardium via interference of focal adhesion complex. Stem Cells 28:555–563.

Sotiropoulou PA, Perez SA, Salagianni M, Baxevanis CN, Papamichail M. 2006. Characterization of the optimal culture conditions for clinical scale production of human mesenchymal stem cells. Stem Cells 24:462–471.

Sun Y, Li WP, Lu ZD, Chen R, Ling J, Ran QT, Jilka RL, Chen XD. 2011. Rescuing replication and osteogenesis of aged mesenchymal stem cells by exposure to a young extracellular matrix. FASEB J 25:1474–1485.

Wang YT, Li J, Wang YM, Lei L, Jiang CM, An S, Zhan YX, Cheng Q, Zhao ZH, Wang J, Jiang LY. 2012. Effects of hypoxia on osteogenic differentiation of rat bone marrow mesenchymal stem cells. Mol Cell Biochem 362: 25–33.

Zaragosi LE, Ailhaud G, Dani C. 2006. Autocrine fibroblast growth factor 2 signaling is critical for self-renewal of human multipotent adipose-derived stem cells. Stem Cells 24:2412–2419.

Zhao F, Grayson WL, Ma T, Irsigler A. 2009. Perfusion affects the tissue developmental patterns of human mesenchymal stem cells in 3D scaffolds. J Cell Physiol 219:421–429.

Zhao F, Ma T. 2005. Perfusion bioreactor system for human mesenchymal stem cell tissue engineering: Dynamic cell seeding and construct development. Biotechnol Bioeng 91:482–493.

Zhao F, Veldhuis JJ, Duan YJ, Yang Y, Christoforou N, Ma T, Leong KW. 2010. Low oxygen tension and synthetic nanogratings improve the uniformity and stemness of human mesenchymal stem cell layer. Mol Ther 18:1010–1018.